

# Tungsten isotopic constraints on the age and origin of chondrules

Gerrit Budde<sup>a,1</sup>, Thorsten Kleine<sup>a</sup>, Thomas S. Kruijjer<sup>a</sup>, Christoph Burkhardt<sup>a</sup>, and Knut Metzler<sup>a</sup>

<sup>a</sup>Institut für Planetologie, University of Muenster, 48149 Muenster, Germany

Edited by Neta A. Bahcall, Princeton University, Princeton, NJ, and approved January 28, 2016 (received for review December 17, 2015)

**Chondrules may have played a critical role in the earliest stages of planet formation by mediating the accumulation of dust into planetesimals. However, the origin of chondrules and their significance for planetesimal accretion remain enigmatic. Here, we show that chondrules and matrix in the carbonaceous chondrite Allende have complementary <sup>183</sup>W anomalies resulting from the uneven distribution of presolar, stellar-derived dust. These data refute an origin of chondrules in protoplanetary collisions and, instead, indicate that chondrules and matrix formed together from a common reservoir of solar nebula dust. Because bulk Allende exhibits no <sup>183</sup>W anomaly, chondrules and matrix must have accreted rapidly to their parent body, implying that the majority of chondrules from a given chondrite group formed in a narrow time interval. Based on Hf-W chronometry on Allende chondrules and matrix, this event occurred ~2 million years after formation of the first solids, about coeval to chondrule formation in ordinary chondrites.**

Hf-W chronometry | nucleosynthetic anomalies | chondrule formation | complementarity | planetesimal accretion

Planet formation is thought to have occurred in stages and involved the collisional growth of kilometer-sized planetesimals to bodies of ever increasing size. However, the first step of planet formation—the initial accumulation of dust into planetesimals—is poorly understood (1, 2). This process can be investigated by studying chondrites, primitive meteorites derived from small bodies that never melted and differentiated. As such, chondrites preserve a record of the physical and chemical processes that affected solid material in the early solar nebula, ultimately leading to the accretion of dust to planetesimals (3). The two major constituents of chondrites are chondrules—micro- to millimeter-sized once-molten silicate spherules—and volatile-rich, fine-grained matrix. Understanding the formation of these two components is key for constraining the origin of chondrites, which in turn may help to identify the processes that led to the accumulation of solar nebula dust into planetesimals. However, the origin of chondrules remains poorly understood, and a wide range of possible formation mechanisms has been proposed: (i) chondrules may have formed through collisions between protoplanetary bodies (4–6); (ii) chondrules may have formed near the Sun and were then transported outward by protostellar jets (7); and (iii) chondrules may have formed through more localized melting events of nebular dust caused by shock waves (8, 9) or current sheets (10). Although many recent models argue for an impact origin of chondrules (4–6), the observation that chondrules and matrix from carbonaceous chondrites are chemically complementary lends strong support to an origin of both components from a single reservoir of nebular dust (11–13). However, the significance of this chemical chondrule–matrix complementarity and whether it can distinguish between a nebular or impact origin of chondrules is debated (6). Thus, not only is the origin of chondrules poorly understood, their importance for making planetesimals is also unclear. Whereas in impact models chondrules formed as a result of the collision of preexisting bodies and, therefore, are only a byproduct of planetary accretion (4–6), a solar nebula origin of chondrules would imply a strong link between chondrule formation and planetesimal accretion (1, 3).

A further complicating factor for constraining the origin of chondrules is that their chronology is not well understood. Although several precise ages for individual chondrules are available (Fig. S1), it remains debated as to whether chondrules from a given chondrite group formed in a narrow time interval or over an extended period lasting several million years (Ma). For instance, precise Pb-Pb ages for individual chondrules from CV3 carbonaceous chondrites range from ~0 to ~3 Ma after formation of Ca-Al-rich inclusions (CAIs), seemingly indicating that chondrules from a given chondrite group formed over a period of at least ~3 Ma (14). However, such a prolonged interval of chondrule formation is inconsistent with the distinct chemical and physical properties of chondrules from a given chondrite group, which seem to require formation of chondrules in a narrow time interval (3). On this basis, some have argued that the range in chondrule ages does not reflect real differences in formation times but at least in part is attributable to parent body alteration (15). Thus, although precise ages for individual chondrules are available, the timescales over which chondrules formed and the significance of the chondrule ages are unclear.

Here, we address these issues using high-precision W isotope measurements on chondrules and matrix separated from the Allende CV3 chondrite. Tungsten isotopes are well suited for constraining the age and origin of chondrules, because W isotope variations may arise (i) through the decay of short-lived <sup>182</sup>Hf to <sup>182</sup>W (half-life = 8.9 Ma), resulting in radiogenic <sup>182</sup>W variations (16), and (ii) through the heterogeneous distribution of the distinct products from the slow (*s*-process) and rapid (*r*-process) neutron capture processes, resulting in nucleosynthetic W isotope anomalies (17). Thus, W isotopes can be used not only to date chondrules but also to assess potential genetic links between distinct chondrite components. For instance, a previous study has

## Significance

**The origin of chondrules—millimeter-sized silicate-rich spherules that dominate the most primitive meteorites, the chondrites—is a long-standing puzzle in cosmochemistry. Here, we present isotopic evidence that chondrules and matrix from the Allende chondrite contain different and complementary proportions of presolar matter, indicating that chondrules and matrix formed together from a single reservoir of solar nebula dust. This finding rules out formation of chondrules in protoplanetary impacts and demonstrates that chondrules are the product of localized melting events in the solar protoplanetary disk. Moreover, the isotopic complementarity of chondrules and matrix requires that chondrules formed in a narrow time interval and were rapidly accreted to a parent body, implying that chondrule formation was a critical step toward forming planetesimals.**

Author contributions: G.B. and T.K. designed research; G.B. performed research; G.B., T.K., T.S.K., C.B., and K.M. analyzed data; and G.B., T.K., T.S.K., C.B., and K.M. wrote the paper.

The authors declare no conflict of interest.

This article is a PNAS Direct Submission.

<sup>1</sup>To whom correspondence should be addressed. Email: gerrit.budde@uni-muenster.de.

This article contains supporting information online at [www.pnas.org/lookup/suppl/doi:10.1073/pnas.1524980113/-DCSupplemental](http://www.pnas.org/lookup/suppl/doi:10.1073/pnas.1524980113/-DCSupplemental).

**Table 1. Hf-W data for Allende chondrules and matrix**

Sample	Normalized to $^{186}\text{W}/^{184}\text{W} = 0.92767$ (6/4)					Normalized to $^{186}\text{W}/^{183}\text{W} = 1.98590$ (6/3)				
	$^{180}\text{Hf}/^{184}\text{W}$ $\pm 2\sigma$	$\epsilon^{182}\text{W}_{\text{meas.}}$ $\pm 2\sigma$	$\epsilon^{183}\text{W}$ $\pm 2\sigma$	$\epsilon^{182}\text{W}_i$ $\pm 2\sigma$	$\epsilon^{182}\text{W}_{\text{nuc. corr.}}$ $\pm 2\sigma$	$\epsilon^{182}\text{W}_{\text{meas.}}$ $\pm 2\sigma$	$\epsilon^{184}\text{W}$ $\pm 2\sigma$	$\epsilon^{182}\text{W}_i$ $\pm 2\sigma$	$\epsilon^{182}\text{W}_{\text{nuc. corr.}}$ $\pm 2\sigma$	
<b>Bulk Allende</b>										
M5-A	$1.328 \pm 0.011$	$-1.97 \pm 0.05$	$0.04 \pm 0.04$	$-3.31 \pm 0.05$	$-2.01 \pm 0.04$	$-1.99 \pm 0.04$	$-0.02 \pm 0.03$	$-3.31 \pm 0.03$	$-1.99 \pm 0.04$	
M5-B	$1.381 \pm 0.008$	$-1.69 \pm 0.03$	$0.17 \pm 0.03$	$-3.08 \pm 0.03$	$-1.90 \pm 0.04$	$-1.90 \pm 0.04$	$-0.12 \pm 0.02$	$-3.27 \pm 0.04$	$-1.89 \pm 0.04$	
<b>Allende matrix</b>										
M1	$0.941 \pm 0.004$	$-4.35 \pm 0.11$	$-1.51 \pm 0.15$	$-5.30 \pm 0.12$	$-2.47 \pm 0.23$	$-2.31 \pm 0.18$	$1.00 \pm 0.10$	$-3.24 \pm 0.18$	$-2.42 \pm 0.19$	
M2	$0.857 \pm 0.004$	$-3.38 \pm 0.11$	$-0.73 \pm 0.15$	$-4.25 \pm 0.12$	$-2.47 \pm 0.22$	$-2.36 \pm 0.18$	$0.49 \pm 0.10$	$-3.21 \pm 0.18$	$-2.41 \pm 0.18$	
M3	$0.920 \pm 0.003$	$-3.72 \pm 0.11$	$-0.98 \pm 0.15$	$-4.65 \pm 0.12$	$-2.50 \pm 0.22$	$-2.38 \pm 0.18$	$0.65 \pm 0.10$	$-3.29 \pm 0.18$	$-2.45 \pm 0.18$	
<b>Allende chondrules</b>										
C1	$2.974 \pm 0.013$	$1.80 \pm 0.11$	$1.79 \pm 0.15$	$-1.20 \pm 0.20$	$-0.43 \pm 0.24$	$-0.56 \pm 0.18$	$-1.19 \pm 0.10$	$-3.51 \pm 0.22$	$-0.43 \pm 0.20$	
C2	$4.451 \pm 0.028$	$2.88 \pm 0.11$	$1.41 \pm 0.15$	$-1.62 \pm 0.27$	$1.12 \pm 0.23$	$0.98 \pm 0.18$	$-0.94 \pm 0.10$	$-3.44 \pm 0.27$	$1.09 \pm 0.19$	
C3m	$3.033 \pm 0.015$	$1.33 \pm 0.11$	$1.39 \pm 0.15$	$-1.73 \pm 0.20$	$-0.39 \pm 0.23$	$-0.53 \pm 0.18$	$-0.92 \pm 0.10$	$-3.53 \pm 0.22$	$-0.42 \pm 0.19$	
C3n	$4.622 \pm 0.031$	$3.97 \pm 0.11$	$2.17 \pm 0.16$	$-0.70 \pm 0.28$	$1.28 \pm 0.26$	$1.11 \pm 0.18$	$-1.44 \pm 0.10$	$-3.47 \pm 0.28$	$1.28 \pm 0.21$	
C3i	$3.351 \pm 0.015$	$2.76 \pm 0.11$	$2.26 \pm 0.15$	$-0.63 \pm 0.22$	$-0.05 \pm 0.25$	$-0.21 \pm 0.18$	$-1.50 \pm 0.10$	$-3.53 \pm 0.23$	$-0.04 \pm 0.21$	
C4	$3.304 \pm 0.024$	$2.57 \pm 0.11$	$2.04 \pm 0.15$	$-0.77 \pm 0.22$	$0.04 \pm 0.25$	$-0.11 \pm 0.18$	$-1.36 \pm 0.10$	$-3.38 \pm 0.23$	$0.05 \pm 0.20$	

Reported W isotope data include measured ( $\epsilon^{182}\text{W}_{\text{meas.}}$ ), decay-corrected ( $\epsilon^{182}\text{W}$ ), and nucleosynthetic anomaly-corrected ( $\epsilon^{182}\text{W}_{\text{nuc. corr.}}$ )  $\epsilon^{182}\text{W}$  values. Uncertainties for bulk Allende (M5-A, M5-B) are 95% CIs defined by repeated analyses of several digestion aliquots. Uncertainties for other samples are based on the external reproducibility of the terrestrial rock standard (Table S2) and include propagated uncertainties induced by the correction for  $^{182}\text{Hf}$  decay and nucleosynthetic isotope anomalies. Further data are provided in Table S3.

shown that chondrules and matrix exhibit complementary Hf/W ratios (18), making it possible to date chondrule formation using the  $^{182}\text{Hf}$ - $^{182}\text{W}$  system. Moreover, several prior studies have shown that nucleosynthetic W isotope anomalies exist in components of primitive chondrites—including CAIs and probably also chondrules (18–20)—but are largely absent from bulk meteorites; thus, W isotopes have much potential as a tracer for the distribution of distinct, isotopically diverse chondrite components at the bulk meteorite and planetary scale. However, although a prior study reported nucleosynthetic W isotope anomalies in Allende chondrules and matrix (18), this study also observed large analytical artifacts on measured W isotope compositions, probably caused by organic interferences on  $^{183}\text{W}$ . Moreover, chondrules and matrix showed both deficits and excesses in  $^{183}\text{W}$ ; this lack of systematic  $^{183}\text{W}$  variations combined with the presence of analytical artifacts makes it difficult to use these data to constrain genetic links between chondrules and matrix. In addition, the presence of nucleosynthetic W isotope anomalies renders precise Hf-W dating of chondrules difficult, resulting in a large uncertainty of  $\sim 3$  Ma for the Hf-W age of CV3 chondrules reported in an earlier study (18). Thus, overall, the magnitude and origin of W isotope anomalies in chondrite components is unclear, and, therefore, the significance of these anomalies for understanding genetic links between these components as well as the mechanisms and timing of chondrule formation has yet to be realized. To address these issues, we used high-precision W isotope measurements on large samples of chondrules and matrix from the Allende chondrite (Table S1).

**Results**

We obtained Hf-W data for three matrix and six chondrule separates as well as for two bulk powders from the Allende chondrite (Supporting Information). The data are reported in  $\epsilon^i\text{W}$  values ( $i = 182, 183, 184$ ) as the parts per 10,000 deviations from terrestrial standard values and are normalized to either the terrestrial  $^{186}\text{W}/^{184}\text{W}$  (termed “6/4” hereafter) or  $^{186}\text{W}/^{183}\text{W}$  (termed “6/3” hereafter) (Table 1). Using these two different normalizations is useful to assess the presence of nucleosynthetic W isotope anomalies, which are much larger for the  $^{186}\text{W}/^{184}\text{W}$  than for the  $^{186}\text{W}/^{183}\text{W}$  normalization (17, 20). This difference arises because  $^{184}\text{W}$  has the largest contribution from the s-process, whereas  $^{182}\text{W}$ ,  $^{183}\text{W}$ , and  $^{186}\text{W}$  all have similar s-process

contributions. The chondrule and matrix samples analyzed display large and complementary  $\epsilon^{183}\text{W}$  anomalies, where all chondrule fractions exhibit elevated  $\epsilon^{183}\text{W}$  (between +1.4 and +2.3), whereas the matrix separates have  $\epsilon^{183}\text{W}$  deficits (from  $-1.5$  to  $-0.7$ ). In contrast, bulk Allende, like other bulk meteorites and inner solar system planets, shows only a small if any  $\epsilon^{183}\text{W}$  anomaly (Fig. 1). Because variations in  $\epsilon^{183}\text{W}$  can only be nucleosynthetic in origin, they indicate different and complementary proportions of presolar material in chondrules and matrix; the matrix with negative  $\epsilon^{183}\text{W}$  is enriched in s-process (or depleted in r-process) W isotopes, whereas the chondrules with positive  $\epsilon^{183}\text{W}$  exhibit a complementary s-deficit (or r-excess).

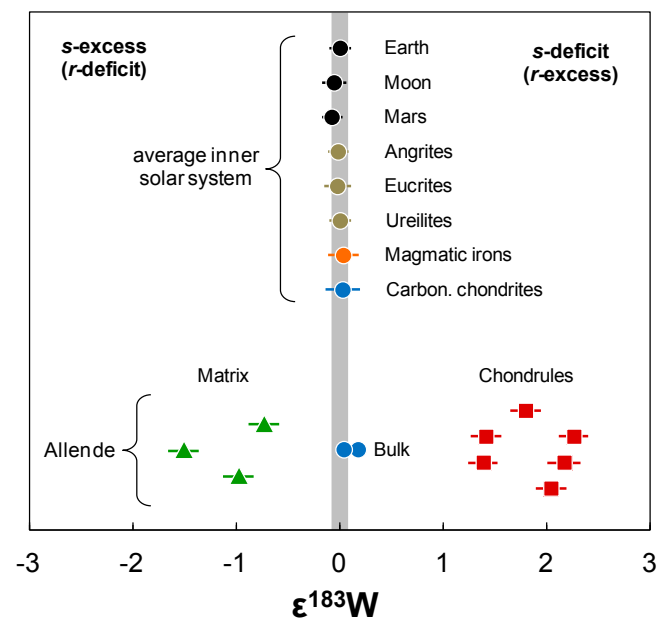


**Fig. 1.**  $\epsilon^{183}\text{W}$  values of meteoritic and planetary samples. Bulk meteorites (32–36) and inner solar system planets [Earth, Moon, Mars (37, 38)] show only small if any nucleosynthetic W isotope anomalies. In contrast, Allende chondrules and matrix show large and complementary  $\epsilon^{183}\text{W}$  variations.

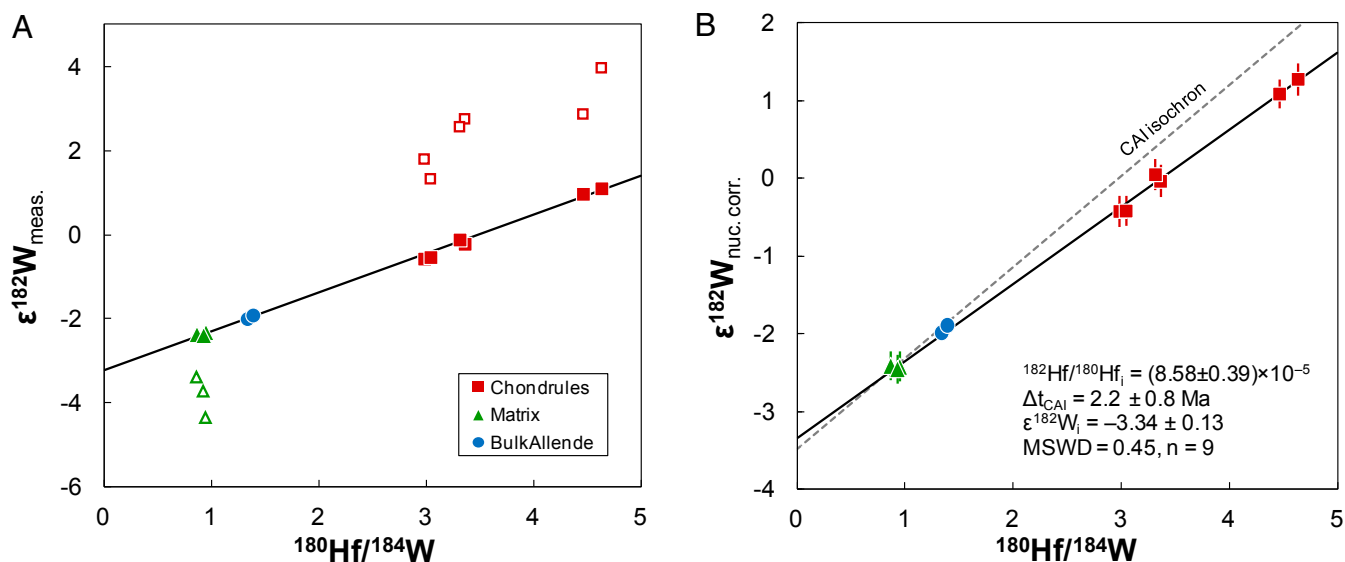


**Fig. 2.** Hf-W isochron for Allende chondrules and matrix. (A) Measured  $\epsilon^{182}\text{W}$  values (open symbols represent 6/4-normalized data, and closed symbols represent 6/3-normalized data). (B)  $\epsilon^{182}\text{W}$  (6/3) values after correction for nucleosynthetic W isotope anomalies. The isochron regression was made using isoplot, and the age of the isochron was calculated relative to  $^{182}\text{Hf}/^{180}\text{Hf} = (1.018 \pm 0.043) \times 10^{-4}$  for CAIs (20). Bulk Allende is shown for comparison and was not included in the isochron regressions (Table S4). Note that the isochron cannot be a mixing line between two distinct end-members (Fig. S2).

In addition to variations in  $\epsilon^{183}\text{W}$ , chondrules and matrix also show complementary anomalies in  $\epsilon^{182}\text{W}$ , with  $^{182}\text{W}$  excesses in chondrules and  $^{182}\text{W}$  deficits in the matrix, relative to bulk Allende. The  $\epsilon^{182}\text{W}$  values of chondrules and matrix are correlated with their  $^{180}\text{Hf}/^{184}\text{W}$  ratios, but only the  $\epsilon^{182}\text{W}$  (6/3) values plot on a single correlation line, defining an Hf-W isochron (Fig. 2A). The  $\epsilon^{182}\text{W}$  (6/4) values show more scatter, consistent with the presence of nucleosynthetic isotope anomalies, which are largest for W isotope ratios involving  $^{184}\text{W}$ . Note that because of the radiogenic  $^{182}\text{W}$  variations, measured  $\epsilon^{182}\text{W}$  and  $\epsilon^{183}\text{W}$  values do not plot on a single correlation line, as would be expected for samples having only nucleosynthetic W isotope anomalies (Fig. S3). Thus, to assess the full magnitude of nucleosynthetic W isotope variations, measured  $\epsilon^{182}\text{W}$  values must first be corrected for radiogenic contributions from the decay of now-extinct  $^{182}\text{Hf}$ . However, this decay correction requires knowledge of the initial  $^{182}\text{Hf}/^{180}\text{Hf}$  of chondrules and matrix, but determining this value in turn requires knowledge of the magnitude of nucleosynthetic  $\epsilon^{182}\text{W}$  variations. (Note that even if the samples would also have nucleosynthetic Hf isotope anomalies, these would be too small to significantly affect  $^{182}\text{Hf}/^{180}\text{Hf}$ , and so the age of the chondrule-matrix isochron must not be known independently for the decay correction.) Thus, both the initial  $^{182}\text{Hf}/^{180}\text{Hf}$  and the slopes of the  $\epsilon^{182}\text{W}(6/4)$ - $\epsilon^{183}\text{W}$  and  $\epsilon^{182}\text{W}(6/3)$ - $\epsilon^{184}\text{W}$  correlation lines must be determined iteratively (for details, see the Supporting Information). This process yields corrected  $\epsilon^{182}\text{W}$  (6/3) and  $\epsilon^{182}\text{W}$  (6/4) values that are indistinguishable (Fig. S4) as well as well-defined correlation lines with a slope of  $1.25 \pm 0.06$  [95% confidence interval (CI);  $n = 9$ ] for  $\epsilon^{182}\text{W}_i$  vs.  $\epsilon^{183}\text{W}$  (6/4) and a slope of  $0.12 \pm 0.07$  for  $\epsilon^{182}\text{W}_i$  vs.  $\epsilon^{184}\text{W}$  (6/3) (Fig. 3A and Fig. S5). These slopes compare well with the range of values calculated from various *s*-process nucleosynthesis models (17) and with data for presolar SiC grains (21) (Fig. 3 and Fig. S5). Thus, the observed nonradiogenic W isotope variations are attributable to the preferential incorporation of an *s*-process carrier into matrix over chondrules (see the Supporting Information for more details about possible carrier phases).

After correction for nucleosynthetic isotope anomalies, chondrules and matrix plot on a single Hf-W isochron, whose slope corresponds to an initial  $^{182}\text{Hf}/^{180}\text{Hf} = (8.58 \pm 0.39) \times 10^{-5}$  (Fig. 2B and

Table S4). Assuming that this isochron has chronological significance, this initial  $^{182}\text{Hf}/^{180}\text{Hf}$  corresponds to an age of  $2.2 \pm 0.8 \text{ Ma}$  after CAI formation. The different  $^{180}\text{Hf}/^{184}\text{W}$  ratios of chondrules and matrix arise through the enrichment of Hf in chondrules and the enrichment of W in matrix (Table S3 and Fig. S6), leading to high Hf/W in chondrules and low Hf/W in matrix. This chemical fractionation is consistent with the general observation (ref. 12 and references therein) that chondrules are enriched in refractory lithophile elements (like Hf), whereas matrix is enriched in siderophile elements (like W), making it possible to date chondrule formation using the Hf-W system. Note that any neutron capture effects on  $^{182}\text{W}$  in the investigated samples are negligible because of the low cosmic ray exposure age of  $\sim 5.2 \text{ Ma}$  for Allende (22), meaning that the observed  $^{182}\text{W}$  variations, after correction for nucleosynthetic effects, can be used to date chondrule formation.

## Discussion

The complementary W isotopic signatures of chondrules and matrix were most likely established during chondrule formation and as such provide critical new insights into possible chondrule formation mechanisms and the timescales of chondrule formation. Prior studies have shown that acid digestion of primitive meteorites does not always lead to complete dissolution of all presolar grains, ultimately affecting measured isotopic compositions (23, 24). For instance, because presolar SiC grains are strongly enriched in *s*-process nuclides (25) and are extremely acid-resistant, a measured *s*-process deficit could reflect the incomplete acid dissolution of *s*-process-enriched SiC grains (23). However, several lines of evidence indicate that the nucleosynthetic  $\epsilon^{183}\text{W}$  variations observed for chondrules and matrix cannot reflect the incomplete dissolution of acid-resistant presolar grains. First, chondrules do not contain presolar grains, and so their elevated  $\epsilon^{183}\text{W}$  cannot result from incomplete dissolution but must be genuine features of the chondrules. Second, incomplete dissolution cannot account for the complementary isotope anomalies in chondrules and matrix, which reflect the enrichment and complementary depletion of a single presolar carrier. Finally, the acid-resistant residue of Allende—which presumably is enriched in presolar grains—has the same  $\epsilon^{183}\text{W}$



from one common reservoir of nebular dust. This finding is consistent with the W isotopic data, because the large and complementary  $\epsilon^{183}\text{W}$  anomalies in chondrules and matrix require that these two components combined result in the average inner solar system  $\epsilon^{183}\text{W}$  observed for bulk meteorites and terrestrial planets (Fig. 1). This observation is most readily explained by forming chondrules and matrix from one common reservoir characterized by  $\epsilon^{183}\text{W} \approx 0$ ; in contrast, it would take extraordinary circumstances for a random mixture of isotopically anomalous chondrules and matrix derived from distinct sources to always result in the inner solar system  $\epsilon^{183}\text{W}$ . Moreover, forming chondrules and matrix from one reservoir of nebular dust can also account for the observed isotopic complementarity, because within this reservoir, presolar dust grains could have been unevenly distributed between chondrules and matrix without changing the  $\epsilon^{183}\text{W}$  of the bulk reservoir. The W isotopic data would be consistent with the heterogeneous distribution of either presolar metal or SiC grains between chondrules and matrix (for details, see [Supporting Information](#)). Thus, one possibility is that presolar grains were separated between chondrules and matrix according to their size or type (metal, silicates, oxides, sulfides). For instance, the matrix is enriched in metal compared with chondrules, and so it is conceivable that presolar metal grains were preferentially incorporated into matrix over chondrules. Alternatively, small presolar grains (e.g., SiC) may have been preferentially excluded from the dust aggregates from which chondrules ultimately formed. Another possibility is that the uneven distribution of presolar material between chondrules and matrix does not reflect the physical separation of grains but is attributable to incomplete melting during chondrule formation. Liquidus temperatures of chondrules are variable and for some if not many chondrules they were below the melting temperatures of SiC and refractory metals (27). Thus, it is conceivable that temperatures during chondrule formation were too low to completely melt refractory presolar grains; these grains would then have been preferentially excluded from the melt that coalesced to form chondrules but would have been enriched in what became the matrix. Thus, the complementary nucleosynthetic isotope anomalies in chondrules and matrix could reflect the incomplete melting of a refractory s-process carrier during chondrule formation. In summary, there is no doubt that solar nebula processes could have led to the observed heterogeneous distribution of presolar matter between chondrules and matrix, even though the details of this process remain uncertain.

After their formation, no (or only very minor) amounts of either chondrules or matrix—both of which have large  $\epsilon^{183}\text{W}$  anomalies—were lost; otherwise, the bulk chondrite would show a significant  $^{183}\text{W}$  anomaly. To prevent this loss in a turbulent solar nebula, where small particles like chondrules would rapidly mix and homogenize (3), it is required that chondrules and matrix accreted rapidly to a chondrite parent body. This requirement is consistent with the distinct physical and chemical properties of chondrules from a given chondrite group, which also indicate that the accretion of chondrules and matrix was fast compared with the mixing timescale of the disk (3). Thus, chondrules from a given chondrite group should be characterized by very similar formation ages; this observation makes it possible to determine the time of chondrule formation using  $^{182}\text{Hf}$ - $^{182}\text{W}$  chronometry, because, owing to the low W contents of individual chondrules, only pooled chondrule separates can be analyzed with sufficient precision ([Supporting Information](#)). After correcting for nucleosynthetic  $\epsilon^{182}\text{W}$  variations, chondrules and matrix define a Hf-W isochron corresponding to an age of  $2.2 \pm 0.8$  Ma after CAI formation (Fig. 2B). This age is significantly more precise and also younger than a recently reported Hf-W age of  $-1.2 \pm 3.0$  Ma after CAIs for Allende chondrules (18). This discrepancy in ages arises from the improper correction of nucleosynthetic W isotope anomalies in the previous study,

leading to spuriously old ages (for details, see the [Supporting Information](#)). Given the large number of chondrules and chondrule fragments analyzed ( $\sim 5,000$ ), the Hf-W age of  $2.2 \pm 0.8$  Ma after CAIs obtained here corresponds to the time at which most Allende chondrules formed. This finding is consistent with Al-Mg ages for individual chondrules from CV and other carbonaceous chondrites (refs. 28 and 29 and references therein), but it is more difficult to reconcile with the range of Pb-Pb ages from  $\sim 0$  to  $\sim 3$  Ma after CAI formation that has been reported for Allende chondrules (14) (Fig. S1). If Allende chondrules indeed would have formed over such an extended period, then the Hf-W isochron, which is based on aggregates of many chondrules, would not necessarily have chronological significance and would at best provide an average age of chondrule formation. However, a prolonged formation interval for chondrules from a single meteorite is inconsistent with the need for rapid accretion of chondrules and matrix to preserve the inner solar system  $\epsilon^{183}\text{W}$  of bulk chondrites (see above). This observation suggests that the Pb-Pb ages reported for Allende chondrules not always reflect the time of chondrule formation or, alternatively, that only a very few Allende chondrules formed as early as CAIs. Either way, the W isotopic data indicate that the vast majority of Allende chondrules formed at  $\sim 2.2$  Ma after CAIs and within a narrow time interval of less than  $\pm 0.6$  Ma (i.e., the uncertainty deriving solely from the scatter on the isochron). As such, our data argue against the recent proposal that the formation of chondrules reflects  $\sim 3$  Ma of continuous thermal processing of solids in the solar accretion disk (14). Finally, because chondrules and matrix accreted rapidly to their parent body, the Hf-W age of  $2.2 \pm 0.8$  Ma after CAI formation closely approximates the time of CV chondrite parent body accretion, in excellent agreement with an accretion age of  $\sim 2.5$  Ma after CAIs inferred from Mn-Cr dating of secondary fayalite in CV chondrites (30).

The W isotope evidence for the formation and subsequent rapid accretion of chondrules and matrix from a single reservoir of nebular dust suggests a close link between chondrule formation and planetesimal accretion. Such a link has previously been proposed based on the observation that the moderately volatile element sodium did not evaporate from chondrule melts, implying that chondrules formed in regions with high solid densities; these regions may have been self-gravitating, ultimately resulting in the accretion of planetesimals (3, 31). These observations combined with the W isotope evidence for rapid accretion of chondrules indicate that chondrule formation not only was associated with strong enrichments of dust but also led to the accumulation of dust to planetesimals, implying that chondrule formation was a critical step toward the formation of planetesimals.

## Materials and Methods

For the present study, we analyzed three matrix and six chondrule separates, which were prepared by freeze-thaw disaggregation or by sieving and hand-picking from a gradually crushed  $\sim 40$ -g slice of the Allende (CV3) chondrite (for details, see the [Supporting Information](#)). The chondrule fractions differ in grain size as well as magnetic susceptibility and comprise between 155 and  $\sim 3,000$  chondrule fragments and intact chondrules. Additionally, two different bulk rock samples of Allende ("MS-A" and "MS-B") were analyzed several times during the course of this study. After digestion of the powdered samples (0.3–0.5 g) with HF-HNO<sub>3</sub>–(HClO<sub>4</sub>) and HNO<sub>3</sub>–HCl mixtures, small aliquots were taken to determine Hf and W concentrations by isotope dilution (ID). The separation of W from the unspiked aliquot for isotope composition (IC) analyses was achieved using a two-stage anion exchange chromatography, and the high-precision W isotope measurements were performed on the Thermo Scientific Neptune Plus multicollector inductively coupled plasma mass spectrometer (MC-ICP-MS) in the Institut für Planetologie at the University of Münster (for details, see the [Supporting Information](#)). The data are reported as  $\epsilon$ -unit deviations (i.e., 0.01%) relative to the bracketing solution standards and were corrected for instrumental mass bias by internal normalization to  $^{186}\text{W}/^{184}\text{W} = 0.92767$  (6/4) or  $^{186}\text{W}/^{183}\text{W} = 1.98590$  (6/3) using the exponential law.

**ACKNOWLEDGMENTS.** We thank an anonymous reviewer, whose detailed and constructive review led to a significant improvement of the paper. We thank Celeste Brennecka for helpful comments that improved the clarity of the paper, Greg Brennecka for detailed discussions, and Mario Fischer-

Gödde and Ursula Heitmann for invaluable technical support. This study was supported by the Deutsche Forschungsgemeinschaft (DFG) as part of the Priority Programme SPP 1385 "The First 10 Million Years of the Solar System—A Planetary Materials Approach" (Grant KL 1857/3).

- Cuzzi JN, Hogan RC, Shariff K (2008) Toward planetesimals: Dense chondrule clumps in the protoplanetary nebula. *Astrophys J* 687(2):1432–1447.
- Johansen A, et al. (2007) Rapid planetesimal formation in turbulent circumstellar disks. *Nature* 448(7157):1022–1025.
- Alexander CMO'D, Grossman JN, Ebel DS, Ciesla FJ (2008) The formation conditions of chondrules and chondrites. *Science* 320(5883):1617–1619.
- Asphaug E, Jutzi M, Movshovitz N (2011) Chondrule formation during planetesimal accretion. *Earth Planet Sci Lett* 308(3–4):369–379.
- Johnson BC, Minton DA, Melosh HJ, Zuber MT (2015) Impact jetting as the origin of chondrules. *Nature* 517(7534):339–341.
- Sanders IS, Scott ERD (2012) The origin of chondrules and chondrites: Debris from low-velocity impacts between molten planetesimals? *Meteorit Planet Sci* 47(12):2170–2192.
- Shu FH, Shang H, Lee T (1996) Toward an astrophysical theory of chondrites. *Science* 271(5255):1545–1552.
- Desch SJ, Ciesla FJ, Hood LL, Nakamoto T (2005) *Chondrites and the Protoplanetary Disk*, eds Krot AN, Scott ERD, Reipurth B (Astronomical Society of the Pacific, San Francisco), pp 849–872.
- Morris MA, Boley AC, Desch SJ, Athanassiadou T (2012) Chondrule formation in bow shocks around eccentric planetary embryos. *Astrophys J* 752(1):27.
- McNally CP, Hubbard A, Mac Low M-M, Ebel DS, D'Alessio P (2013) Mineral processing by short circuits in protoplanetary disks. *Astrophys J* 767(1):L2.
- Bland PA, et al. (2005) Volatile fractionation in the early solar system and chondrule/matrix complementarity. *Proc Natl Acad Sci USA* 102(39):13755–13760.
- Palme H, Hezel DC, Ebel DS (2015) The origin of chondrules: Constraints from matrix composition and matrix-chondrule complementarity. *Earth Planet Sci Lett* 411:11–19.
- Ebel DS, et al. (2016) Abundance, major element composition and size of components and matrix in CV, CO and Acfer 094 chondrites. *Geochim Cosmochim Acta* 172:322–356.
- Connelly JN, et al. (2012) The absolute chronology and thermal processing of solids in the solar protoplanetary disk. *Science* 338(6107):651–655.
- Alexander CMO'D, Ebel DS (2012) Questions, questions: Can the contradictions between the petrologic, isotopic, thermodynamic, and astrophysical constraints on chondrule formation be resolved? *Meteorit Planet Sci* 47(7):1157–1175.
- Kleine T, et al. (2009) Hf–W chronology of the accretion and early evolution of asteroids and terrestrial planets. *Geochim Cosmochim Acta* 73(17):5150–5188.
- Burkhardt C, Schönbächler M (2015) Intrinsic W nucleosynthetic isotope variations in carbonaceous chondrites: Implications for W nucleosynthesis and nebular vs. parent body processing of presolar materials. *Geochim Cosmochim Acta* 165:361–375.
- Becker M, Hezel DC, Schulz T, Elfers B-M, Münker C (2015) Formation timescales of CV chondrites from component specific Hf–W systematics. *Earth Planet Sci Lett* 432:472–482.
- Burkhardt C, et al. (2008) Hf–W mineral isochron for Ca,Al-rich inclusions: Age of the solar system and the timing of core formation in planetesimals. *Geochim Cosmochim Acta* 72(24):6177–6197.
- Kruijjer TS, Kleine T, Fischer-Gödde M, Burkhardt C, Wieler R (2014) Nucleosynthetic W isotope anomalies and the Hf–W chronometry of Ca–Al-rich inclusions. *Earth Planet Sci Lett* 403:317–327.
- Ávila JN, et al. (2012) Tungsten isotopic compositions in stardust SiC grains from the Murchison meteorite: Constraints on the s-process in the Hf-Ta-W-Re-Os region. *Astrophys J* 744(1):49.
- Scherer P, Schultz L (2000) Noble gas record, collisional history, and pairing of CV, CO, CK, and other carbonaceous chondrites. *Meteorit Planet Sci* 35(1):145–153.
- Brandon AD, Humayun M, Puchtel IS, Leya I, Zolensky M (2005) Osmium isotope evidence for an s-process carrier in primitive chondrites. *Science* 309(5738):1233–1236.
- Yokoyama T, et al. (2007) Osmium isotope evidence for uniform distribution of s- and r-process components in the early solar system. *Earth Planet Sci Lett* 259(3–4):567–580.
- Hoppe P, Ott U (1997) Mainstream silicon carbide grains from meteorites. *AIP Conf Proc* 402:27–58.
- Yokoyama T, Alexander CMO'D, Walker RJ (2011) Assessment of nebular versus parent body processes on presolar components present in chondrites: Evidence from osmium isotopes. *Earth Planet Sci Lett* 305(1–2):115–123.
- Cohen BA, Hewins RH, Yu Y (2000) Evaporation in the young solar nebula as the origin of 'just-right' melting of chondrules. *Nature* 406(6796):600–602.
- Luu T-H, Young ED, Gounelle M, Chaussidon M (2015) Short time interval for condensation of high-temperature silicates in the solar accretion disk. *Proc Natl Acad Sci USA* 112(5):1298–1303.
- Ushikubo T, Nagashima K, Kimura M, Tenner TJ, Kita NT (2013) Contemporaneous formation of chondrules in distinct oxygen isotope reservoirs. *Geochim Cosmochim Acta* 109:280–295.
- Doyle PM, et al. (2015) Early aqueous activity on the ordinary and carbonaceous chondrite parent bodies recorded by fayalite. *Nat Commun* 6:7444.
- Cuzzi JN, Alexander CM (2006) Chondrule formation in particle-rich nebular regions at least hundreds of kilometres across. *Nature* 441(7092):483–485.
- Kleine T, Hans U, Irving AJ, Bourdon B (2012) Chronology of the angrite parent body and implications for core formation in protoplanets. *Geochim Cosmochim Acta* 84:186–203.
- Touboul M, Sprung P, Aciego SM, Bourdon B, Kleine T (2015) Hf–W chronology of the eucrite parent body. *Geochim Cosmochim Acta* 156:106–121.
- Budde G, Kruijjer TS, Fischer-Gödde M, Kleine T (2015) Planetesimal differentiation revealed by the Hf–W systematics of ureilites. *Earth Planet Sci Lett* 430:316–325.
- Kruijjer TS, et al. (2014) Protracted core formation and rapid accretion of protoplanets. *Science* 344(6188):1150–1154.
- Kleine T, Mezger K, Münker C, Palme H, Bischoff A (2004) <sup>182</sup>Hf-<sup>182</sup>W isotope systematics of chondrites, eucrites, and martian meteorites: Chronology of core formation and early mantle differentiation in Vesta and Mars. *Geochim Cosmochim Acta* 68(13):2935–2946.
- Kruijjer TS, Kleine T, Fischer-Gödde M, Sprung P (2015) Lunar tungsten isotopic evidence for the late veneer. *Nature* 520(7548):534–537.
- Kruijjer TS, et al. High-precision <sup>182</sup>W measurements of Martian meteorites for constraining the early evolution of Mars. Forty-Sixth Lunar Planetary Science Conference, March 16–20, 2015, Houston, abstr 1928.
- Kleine T, Münker C, Mezger K, Palme H (2002) Rapid accretion and early core formation on asteroids and the terrestrial planets from Hf–W chronometry. *Nature* 418(6901):952–955.
- Kruijjer TS, et al. (2012) Hf–W chronometry of core formation in planetesimals inferred from weakly irradiated iron meteorites. *Geochim Cosmochim Acta* 99:287–304.
- Lugaro M, et al. (2014) Early solar system. Stellar origin of the <sup>182</sup>Hf cosmochronometer and the presolar history of solar system matter. *Science* 345(6197):650–653.
- Vockenhuber C, et al. (2004) New half-life measurement of <sup>182</sup>Hf: Improved chronometer for the early solar system. *Phys Rev Lett* 93(17):172501.
- Cody GD, et al. (2008) Organic thermometry for chondritic parent bodies. *Earth Planet Sci Lett* 272(1–2):446–455.
- Kleine T, et al. (2008) Hf–W thermochronometry: Closure temperature and constraints on the accretion and cooling history of the H chondrite parent body. *Earth Planet Sci Lett* 270(1–2):106–118.
- Brennecka GA, Budde G, Kleine T (2015) Uranium isotopic composition and absolute ages of Allende chondrules. *Meteorit Planet Sci* 50(12):1995–2002.

# Supporting Information

Budde et al. 10.1073/pnas.1524980113

## S1. SI Materials and Methods

**S1.1. Sample Preparation.** In CV chondrites, chondrules have typical a diameter of 250–1500  $\mu\text{m}$  and  $\sim 90\%$  are type I (FeO-poor) porphyritic (mainly porphyritic olivine) chondrules. In the case of Allende (CV3<sub>OX</sub>), chondrules are together with other components [CAIs, amoeboid olivine aggregates (AOAs)] embedded in a matrix of fine-grained silicates, oxides, and sulfides. For the present study, we analyzed two different bulk rock samples of the Allende meteorite (MS-A, MS-B), six chondrule fractions, and three matrix separates. The two bulk rock powders were prepared by grinding two large slabs of Allende ( $\sim 100$  g in case of MS-A;  $\sim 40$  g in case of MS-B) in a vibratory disk mill equipped with an agate vessel and were analyzed several times during the course of this study. The chondrule and matrix samples were prepared using different techniques that are described in detail in the following paragraphs (Table S1).

One matrix fraction and one chondrule fraction were prepared by the freeze–thaw disaggregation technique. A small piece of Allende ( $\sim 4.2$  g) was carefully cleaned by polishing with  $\text{Al}_2\text{O}_3$  and sonication in acetone. After immersing in ultrapure water, the sample was disaggregated by 200 freeze–thaw cycles, which included freezing in liquid nitrogen and thawing in an ultrasonic bath. Because matrix material is very fine-grained, it is finely dispersed in the water and thus the suspension was decanted and centrifuged to recover the matrix fraction (M1), which was then dried at room temperature. The chondrule separate (C1) was hand-picked from the coarser disaggregated material (250–1600  $\mu\text{m}$ ). The other chondrule and matrix fractions were prepared from a larger slice of Allende ( $\sim 40$  g), which was cut into smaller pieces using a diamond saw. After removing large CAIs with an  $\text{Al}_2\text{O}_3$  drill, the sample was carefully cleaned by polishing with SiC and sonication in acetone. The pieces were then gradually crushed in an agate mortar and sieved using polyamide meshes. Chondrules and chondrule fragments of three different grain size fractions (1,000–1,600; 500–1,000; 250–500  $\mu\text{m}$ ) with a total weight of  $\sim 2.4$  g were hand-picked (C2, C3, C4). The intermediate grain size fraction was then further separated into three fractions according to their magnetic susceptibility using a hand magnet (C3m, C3i, C3n). An additional matrix separate (M2) was prepared by careful hand-picking from a 250–500- $\mu\text{m}$  grain size fraction, whereas a third matrix fraction (M3) was obtained from crushed material (250–1,000  $\mu\text{m}$ ) that was free from any visible chondrule or CAI material. This sample was sonicated in ethanol for  $\sim 10$  h, followed by decanting and centrifuging the suspension to recover the matrix separate (M3).

All chondrule fractions were carefully purified by hand-picking under the stereo microscope, and their purity was cross-checked by two of the authors involved in this study. After sonication in acetone for further cleaning, the chondrule separates were ground to a fine powder in an agate mortar. Depending on the grain size and weight, each fraction consists of 155 to  $\sim 3,000$  chondrule fragments and intact chondrules. Although the purity of the chondrule separates could be monitored, it is more difficult to assess the purity of the matrix separates. However, our data show that the matrix fractions prepared in three different ways yield consistent results, strongly suggesting that the contribution of components other than matrix material is minor.

**S1.2. Chemical Separation and W Isotope Measurements.** Bulk Allende as well as the matrix separates (0.4–0.5 g) were digested in Savillex beakers on a hotplate using a  $\text{HF-HNO}_3\text{-HClO}_4$  (2:1:0.01) mixture at 180  $^\circ\text{C}$  (5 d), followed by inverse aqua regia

at 130–150  $^\circ\text{C}$  (2 d). To minimize a potential W contamination from the digestion vials, chondrule fractions (0.3–0.5 g) were digested with a  $\text{HF-HNO}_3$  (2:1) mixture at 130  $^\circ\text{C}$  (3 d) and inverse aqua regia at 110  $^\circ\text{C}$  (1 d). After repeated dry-downs and complete dissolution in 6 M  $\text{HCl}$ –0.06 M  $\text{HF}$ , small aliquots ( $\sim 2\%$ ) were taken to determine Hf and W concentrations by ID. The ID aliquots (equivalent to  $\sim 1$ –3 ng W and Hf) were spiked with a mixed  $^{180}\text{Hf}$ – $^{183}\text{W}$  tracer that was calibrated against pure Hf and W metal standards (36, 39). The chemical separation of Hf and W by anion-exchange chromatography for ID analyses followed ref. 36.

The separation of W from the unspiked aliquot for IC analyses was performed using a two-stage anion-exchange chromatography slightly modified after refs. 32 and 40. The sample aliquots were loaded in 75 mL of 0.5 M  $\text{HCl}$ –0.5 M  $\text{HF}$  onto columns filled with 4 mL of precleaned Bio-Rad AG1-X8 anion exchange resin (200–400 mesh). Most of the sample matrix was washed off the column with the loading solution and additional 10 mL of 0.5 M  $\text{HCl}$ –0.5 M  $\text{HF}$ , followed by elution of W in 15 mL 6 M  $\text{HCl}$ –1 M  $\text{HF}$ . After drying, the samples were dissolved in 6 mL of 0.6 M  $\text{HF}$ –0.4%  $\text{H}_2\text{O}_2$  and loaded onto a clean-up column containing 1 mL of precleaned AG1-X8 resin. The columns were then rinsed with 10 mL of 1 M  $\text{HCl}$ –2%  $\text{H}_2\text{O}_2$ , 9 mL of 8 M  $\text{HCl}$ –0.01 M  $\text{HF}$ , and 0.5 mL of 6 M  $\text{HCl}$ –1 M  $\text{HF}$  to quantitatively remove the HFSE (Ti, Zr, Hf, Ta), followed by elution of W with 8.5 mL 6 M  $\text{HCl}$ –1 M  $\text{HF}$ . The W cuts from both ion-chromatography steps were evaporated at 200  $^\circ\text{C}$  with added  $\text{HClO}_4$  to destroy organic compounds. The W yield for this two-column procedure was typically  $\sim 70\%$ . Total procedural blanks for the IC measurements ranged from 50 to 70 pg of W (chondrules) to 100–300 pg (bulk rock, matrix) and were negligible. Typical blanks for the Hf and W ID analyses were  $\sim 13$  pg of Hf and  $\sim 11$  pg of W, respectively. The blank corrections for the ID analyses were  $<2\%$  and included in the uncertainty of the  $^{180}\text{Hf}/^{184}\text{W}$  assuming an average uncertainty on the blank correction of 50%.

The W isotope measurements were performed on the Thermo Scientific Neptune Plus MC-ICP-MS in the Institut für Planetologie at the University of Münster and followed the measurement protocols described in ref. 20. The samples were introduced into the mass spectrometer using an ESI PFA nebulizer connected to a Cetac Aridus II desolvator. A combination of Jet sampler and X skimmer cones was used, and the data were corrected for instrumental mass bias by internal normalization to  $^{186}\text{W}/^{184}\text{W} = 0.92767$  (6/4) or  $^{186}\text{W}/^{183}\text{W} = 1.98590$  (6/3) using the exponential law. Each analysis consisted of 60-s baseline measurements (deflected beam), followed by 200 isotope ratio measurements of 4.2 s each and consumed about 30 ng of W. Possible isobaric interferences of Os on  $^{184}\text{W}$  and  $^{186}\text{W}$  were corrected by monitoring interference-free  $^{188}\text{Os}$  and were negligible for all analyzed samples. The W isotope data are reported as  $\epsilon$ -unit deviations (i.e., 0.01%) relative to the bracketing Alfa Aesar solution standards [prepared from a pure W metal; batch no. 22312 (36, 39)]. For samples analyzed several times, the reported values represent the mean of pooled solution replicates. The accuracy and precision of the W isotope measurements were evaluated by repeated analyses of the BHVO-2 rock standard (Table S2). The BHVO-2 ( $\sim 0.5$  g per digestion) powder was processed through the full chemical separation and analyzed together with each set of samples. The mean  $\epsilon^{182}\text{W}$  (6/4) of  $-0.02 \pm 0.11$  (2 SD;  $n = 29$ ) obtained during the course of this study is indistinguishable from the W isotope composition of the Alfa Aesar standard. As observed in previous high-precision W isotope studies (20, 34, 35), normalizations

involving  $^{183}\text{W}$  show a small mass-independent effect ( $\sim 0.1 \epsilon$  units) for the terrestrial standard that was corrected after ref. 40. For the Allende samples, we corrected all  $\epsilon^{181}\text{W}$  values involving  $^{183}\text{W}$  using the mean values obtained for the BHVO-2 standard, and the associated uncertainties were propagated into the final uncertainty reported for the W isotope data. We note that the nucleosynthetic W isotope anomalies observed for chondrule and matrix fractions are one order of magnitude larger than and thus clearly resolved from the small  $^{183}\text{W}$  effects observed during mass spectrometric analyses.

The Hf and W concentration and high-precision W isotope data obtained for six chondrule fractions, three matrix separates, and two different bulk Allende powders are provided in Table 1 and Table S3. Additional data for the terrestrial rock standard BHVO-2, which defines the external reproducibility of our analytical method, is given in Table S2. Note that the reported uncertainties include all propagated uncertainties induced by the correction for the mass-independent effect, radiogenic contributions from  $^{182}\text{Hf}$  decay, and nucleosynthetic isotope anomalies, respectively.

## 52. SI Text

**52.1. Hf-W Isotope Systematics of Allende Chondrules and Matrix.** Lithophile Hf and siderophile W should have been strongly fractionated between chondrules and matrix, because chondrules are enriched in lithophile elements, whereas the matrix is enriched in siderophile elements (11, 12, 18). This chemical Hf-W complementarity between chondrules and matrix makes it possible to date chondrule formation using the  $^{182}\text{Hf}$ - $^{182}\text{W}$  system (S2. SI Text, S2.4. Isochron Regression and Chronological Significance). Consistent with previous studies on the chemical complementarity of chondrules and matrix, the matrix separates analyzed in this study are enriched in W ( $\sim 197$  ppb) relative to bulk Allende, whereas Hf ( $\sim 151$  ppb) is depleted in the matrix. The chondrule fractions show a complementary chemical signature (Fig. S6), where W concentrations range from 71 ppb (nonmagnetic fraction) to 110 ppb (magnetic fraction). Note that when recombining the magnetic separates (of fraction “C3”), the different grain size fractions show only small variations in W concentrations (Table S3). In contrast, Hf contents are much more variable (230–341 ppb) among the chondrule fractions and positively correlated with their grain size. This variability leads to a significant spread in Hf/W ratios, where chondrules have higher-than-chondritic  $^{180}\text{Hf}/^{184}\text{W}$ , ranging from  $\sim 3.0$  to  $\sim 4.6$ , whereas the matrix exhibits a complementary lower-than-chondritic ratio of  $\sim 0.9$  (Fig. 2). Note that even without magnetic separation (of fraction C3), a significant spread in Hf/W ratios among the chondrule fractions exists because of large variations in their Hf concentrations.

The matrix and chondrules samples exhibit complementary  $\epsilon^{183}\text{W}$  anomalies, where the matrix separates have  $\epsilon^{183}\text{W}$  (6/4) deficits of about  $-1.5$  to  $-0.7$ , whereas the chondrule fractions have variable excesses between  $+1.4$  and  $+2.3$ . These  $\epsilon^{183}\text{W}$  variations cannot reflect the incomplete dissolution of acid-resistant presolar grains, because such an incomplete digestion cannot account for the complementary isotope anomalies in chondrules and matrix (see Discussion). Moreover, the acid-resistant residue of Allende has the same  $\epsilon^{183}\text{W}$  anomaly than measured here for matrix-enriched samples (17), indicating that exclusion of such acid-resistant material could not result in the isotope anomalies measured for the matrix samples. Finally, the  $\epsilon^{183}\text{W}$  excesses observed for chondrules are also unlikely to result from the incorporation of CAI material during chondrule formation, because most CAIs have much smaller (if any)  $\epsilon^{183}\text{W}$  anomalies than observed here for chondrules (20). Thus, the  $\epsilon^{183}\text{W}$  variations are characteristic for chondrules and matrix in Allende. Note that although the chondrule fractions consist of 155 to  $\sim 3,000$  chondrules and chondrule fragments, the fractions show significant

variations in  $\epsilon^{183}\text{W}$ , implying that the variations between individual chondrules might be even larger.

The matrix separates exhibit subchondritic  $\epsilon^{182}\text{W}$  (6/4) ranging from  $-4.4$  to  $-3.4$ , whereas their  $\epsilon^{182}\text{W}$  (6/3) of about  $-2.4$  are indistinguishable (Fig. S3). In contrast, the chondrule fractions have superchondritic  $\epsilon^{182}\text{W}$  (6/4) ranging from 1.3 to 4.0, whereas their  $\epsilon^{182}\text{W}$  (6/3) are much less variable and between  $-0.6$  and 1.1. As expected, the differences in  $\epsilon^{182}\text{W}$  between the two normalizations scale with the magnitude of anomalies in  $\epsilon^{183}\text{W}$ . Note that any neutron capture effects on  $^{182}\text{W}$  in the investigated samples are negligible because of the low cosmic ray exposure age of  $\sim 5.2$  Ma for Allende (22). Both the  $\epsilon^{182}\text{W}$  (6/4) and  $\epsilon^{182}\text{W}$  (6/3) values of the investigated samples show a positive correlation with the corresponding  $^{180}\text{Hf}/^{184}\text{W}$  ratios (Fig. 2A). However, this correlation is much better defined in the case of the 6/3-normalized values, reflecting that the  $\epsilon^{182}\text{W}$  values obtained by the different normalizations are distinct.

The Hf-W data for bulk Allende (MS-A) is in excellent agreement with previous data obtained for the same powder (20) and shows that bulk Allende has only a small if any anomaly in  $\epsilon^{183}\text{W}$  relative to the terrestrial value. The MS-A powder was prepared from a  $\sim 100$ -g slab of Allende and is probably more representative than the MS-B powder, which shows a small excess in  $\epsilon^{183}\text{W}$  that is resolved from the terrestrial value. The latter was prepared from a smaller slab of Allende ( $\sim 40$  g) and may have a slight overabundance of chondrules or fine-grained CAIs, resulting in an elevated  $\epsilon^{183}\text{W}$ . Regardless of this finding, the overall effect of CAIs on the  $\epsilon^{183}\text{W}$  composition of bulk Allende is small (resulting in much smaller variations than observed here for chondrules and matrix), because most bulk CAIs show only a small if any  $\epsilon^{183}\text{W}$  anomaly (20).

**52.2. Nucleosynthetic and Radiogenic Contributions to Measured  $\epsilon^{182}\text{W}$  Variations.** Allende matrix and chondrules display large nucleosynthetic W isotope anomalies, as is evident from their non-terrestrial  $\epsilon^{183}\text{W}$  values. These nucleosynthetic variations reflect a heterogeneous distribution of *s*- or *r*-process W nuclides and—in addition to causing variable  $\epsilon^{183}\text{W}$ —also lead to disparate  $\epsilon^{182}\text{W}$  (6/3) and  $\epsilon^{182}\text{W}$  (6/4) anomalies, because the magnitude of this effect on the measured  $\epsilon^{182}\text{W}$  depends on the internal normalization applied to correct for instrumental mass bias (17, 19, 20). For instance, values normalized to  $^{186}\text{W}/^{183}\text{W}$  (6/3) are only marginally affected by nucleosynthetic isotope variability, whereas the effect on isotope ratios normalized to  $^{186}\text{W}/^{184}\text{W}$  (6/4) is substantial (17, 19, 20). In contrast to  $\epsilon^{183}\text{W}$ , the variations in  $\epsilon^{182}\text{W}$  are not only nucleosynthetic in origin but also reflect the decay of now-extinct  $^{182}\text{Hf}$ . Thus, distinguishing nucleosynthetic from radiogenic contributions to observed  $^{182}\text{W}$  variations requires quantifying both effects. However, although the correction for nucleosynthetic  $\epsilon^{182}\text{W}$  variations can be accomplished using the linear relationship between  $\epsilon^{182}\text{W}$  and  $\epsilon^{183}\text{W}$  (or  $\epsilon^{184}\text{W}$ ) combined with the measured  $\epsilon^{183}\text{W}$  (or  $\epsilon^{184}\text{W}$ ) anomaly of each sample, obtaining the  $\epsilon^{182}\text{W}$ - $\epsilon^{183}\text{W}$  (and  $\epsilon^{182}\text{W}$ - $\epsilon^{184}\text{W}$ ) slopes requires the prior correction of the measured  $\epsilon^{182}\text{W}$  for radiogenic contributions from  $^{182}\text{Hf}$  decay. However, the latter requires knowledge of the initial  $^{182}\text{Hf}/^{180}\text{Hf}$  of chondrules and matrix, a parameter we ultimately want to determine from the isochron after correction for nucleosynthetic W isotope variations.

We, therefore, determined the  $\epsilon^{182}\text{W}$ - $\epsilon^{183}\text{W}$  (and  $\epsilon^{182}\text{W}$ - $\epsilon^{184}\text{W}$ ) slopes as well as the initial  $^{182}\text{Hf}/^{180}\text{Hf}$  of the chondrule-matrix isochron through an iterative procedure after ref. 20: first, we corrected the measured  $\epsilon^{182}\text{W}$  values for radiogenic contributions using their measured  $^{180}\text{Hf}/^{184}\text{W}$  and the initial  $^{182}\text{Hf}/^{180}\text{Hf}$  provided by the isochron regression of the measured  $\epsilon^{182}\text{W}$  (6/3) values. These values already show a well-defined correlation with  $^{180}\text{Hf}/^{184}\text{W}$  and thus provide a reasonable estimate of the initial  $^{182}\text{Hf}/^{180}\text{Hf}$  of the chondrule-matrix isochron (Fig. 2A); this finding reflects the only small effects of nucleosynthetic W isotope

variations on isotope ratios normalized to  $^{186}\text{W}/^{183}\text{W}$  (see *Results*). The decay-corrected  $\epsilon^{182}\text{W}$  values ( $\epsilon^{182}\text{W}_i$ ) thus obtained are linearly correlated with the  $\epsilon^{183}\text{W}$  (and  $\epsilon^{184}\text{W}$ ), and the slopes of the  $\epsilon^{182}\text{W}-\epsilon^{183}\text{W}$  and  $\epsilon^{182}\text{W}-\epsilon^{184}\text{W}$  correlation lines can be used to correct measured  $\epsilon^{182}\text{W}$  values for nucleosynthetic isotope variations. Linear regression of the corrected  $\epsilon^{182}\text{W}$  values thus obtained then provides an improved estimate for the initial  $^{182}\text{Hf}/^{180}\text{Hf}$  of the chondrule–matrix isochron. With this new estimate, the entire procedure is repeated until both the slopes of the  $\epsilon^{182}\text{W}-\epsilon^{183}\text{W}$  and  $\epsilon^{182}\text{W}-\epsilon^{184}\text{W}$  correlation lines as well as the initial  $^{182}\text{Hf}/^{180}\text{Hf}$  obtained for the nucleosynthetic anomaly-corrected  $\epsilon^{182}\text{W}$  data remain constant. This process yields corrected  $\epsilon^{182}\text{W}$  (6/3) and  $\epsilon^{182}\text{W}$  (6/4) values that are indistinguishable (Fig. S4) as well as well-defined correlation lines with a slope of  $1.25 \pm 0.06$  (95% CI;  $n = 9$ ) for  $\epsilon^{182}\text{W}_i$  vs.  $\epsilon^{183}\text{W}$  (6/4) and a slope of  $0.12 \pm 0.07$  for  $\epsilon^{182}\text{W}_i$  vs.  $\epsilon^{184}\text{W}$  (6/3) (Fig. 3A and Fig. S5). Note that all uncertainties introduced by this correction procedure were propagated into the corrected  $\epsilon^{182}\text{W}$  data.

**S2.3. Origin of Nucleosynthetic W Isotope Variations Between Chondrules and Matrix.** The  $\epsilon^{182}\text{W}-\epsilon^{183}\text{W}$  and  $\epsilon^{182}\text{W}-\epsilon^{184}\text{W}$  slopes obtained after the iterative procedure described above (S2. SI Text, S2.2. *Nucleosynthetic and Radiogenic Contributions to Measured  $\epsilon^{182}\text{W}$  Variations*) compare well with the range of values calculated from various *s*-process nucleosynthesis models (17), indicating that the observed W isotope variations are attributable to the heterogeneous distribution of *s*-process matter (Fig. 3). Note, however, that the opposite—the heterogeneous distribution of an *r*-process carrier—cannot be excluded based on the W isotopic data alone. Compared with chondrules and matrix, slightly different  $\epsilon^{182}\text{W}_i(6/4)-\epsilon^{183}\text{W}(6/4)$  and  $\epsilon^{182}\text{W}_i(6/3)-\epsilon^{184}\text{W}(6/3)$  slopes of  $1.41 \pm 0.06$  and  $-0.11 \pm 0.05$  were obtained for CAIs (20), indicating that the nucleosynthetic W isotope anomalies in chondrules–matrix and CAIs are caused by different presolar carriers. Presolar SiC grains (21) plot on the  $\epsilon^{182}\text{W}(6/4)-\epsilon^{183}\text{W}(6/4)$  correlation defined by chondrules and matrix (Fig. 3B), suggesting that Allende matrix is enriched in SiC over chondrules. However, acid residues from both Orgueil and Murchison are both enriched in SiC, but the residues' W isotopic signatures are more compatible with a  $\epsilon^{182}\text{W}(6/4)-\epsilon^{183}\text{W}(6/4)$  slope of 1.41 than 1.25 (17). Of note, an acid-soluble *s*-process carrier with  $\epsilon^{182}\text{W}/\epsilon^{183}\text{W} \sim 1.25$  has been identified by mild leaching of Orgueil (17). Given that this carrier is soluble in nitric acid, it could be metal or sulfide. Such a carrier would have a very low Hf/W and would, therefore, be deficient in *s*-process  $^{182}\text{W}$  produced through decay of  $^{182}\text{Hf}$  (41). This finding in turn would be consistent with the lower  $\epsilon^{182}\text{W}/\epsilon^{183}\text{W}$  of  $\sim 1.25$  of this component compared with a value of  $\sim 1.41$  observed for the acid residues. Nevertheless, the exact nature of this presolar carrier phase remains uncertain, and further isotope measurements using both lithophile and siderophile elements are needed to more definitely identify its nature.

**S2.4. Isochron Regression and Chronological Significance.** After correction of measured  $\epsilon^{182}\text{W}$  values for nucleosynthetic W isotope anomalies, all matrix and chondrule fractions plot on a well-defined isochron (Fig. 2B). Both normalizations yield consistent results, but the precision of the 6/3-normalized values is generally better because of much smaller corrections for nucleosynthetic W isotope anomalies (Fig. S4). Thus, we used the corrected  $\epsilon^{182}\text{W}$  (6/3) values for the isochron regression, for which only the three matrix and six chondrule fractions were considered. The regression was calculated using the Model 1 fit of Isoplot (version 3.76) and yields an initial  $^{182}\text{Hf}/^{180}\text{Hf}$  of  $(8.58 \pm 0.39) \times 10^{-5}$  and an initial  $\epsilon^{182}\text{W}$  of  $-3.34 \pm 0.13$  (95% CI;  $n = 9$ ). Relative to the initial  $^{182}\text{Hf}/^{180}\text{Hf} = (1.018 \pm 0.043) \times 10^{-4}$  of CAIs (20), the  $^{182}\text{Hf}/^{180}\text{Hf}$  obtained from the chondrule–matrix isochron corresponds to a Hf–W age of  $2.2 \pm 0.8$  Ma after CAI formation [using  $\lambda(^{182}\text{Hf}) = 0.0778 \pm 0.0015 \text{ Ma}^{-1}$  (42)]. This age is consis-

tent with the  $\epsilon^{182}\text{W}_i$  of  $-3.34 \pm 0.13$  that is higher than (albeit not resolved from) the solar system initial of  $-3.49 \pm 0.07$  as inferred from CAIs (20). Results for other isochron regressions are shown in Table S4.

The absence of a well-defined linear correlation between  $\epsilon^{182}\text{W}$  and 1/W indicates that the chondrule–matrix isochron has chronological significance and is not a mixing line between two distinct end-members, which could potentially have formed at different times (Fig. S2). As noted above, bulk Allende was not included in the isochron regression because it contains CAIs with different Hf–W systematics; however, bulk Allende plots exactly on the chondrule–matrix isochron. This result is not surprising because most CAIs have  $^{180}\text{Hf}/^{184}\text{W}$  and  $\epsilon^{182}\text{W}$  values quite similar to those of bulk chondrites (including Allende). Thus, the addition of CAIs to bulk chondrites has little effect on the overall Hf–W systematics of the bulk rock. Nevertheless, some bulk CAIs show a large spread in  $\epsilon^{182}\text{W}$  and  $^{180}\text{Hf}/^{184}\text{W}$  and define an isochron that is distinct from the matrix–chondrule isochron (Fig. 2B). This isochron is mainly defined by fine-grained CAIs, however, and these typically have lower W contents and, hence, little effect on the Hf–W systematics of bulk Allende (20).

**S2.5. Effects of Parent Body Processes on W Isotope Systematics.** The Allende meteorite has experienced low-grade thermal metamorphism and aqueous alteration on its parent body, raising the question of whether these processes affected the W isotope systematics of its components. However, the complementary W isotopic signatures observed for chondrules and matrix are not the result of parent body processes but are genuine features of these two components established during chondrule formation (see *Discussion*). For example, the preservation of complementary nucleosynthetic W isotope anomalies in chondrules and matrix implies that there was minimal diffusional exchange between these two components during parent body processes. This finding is consistent with the peak metamorphic temperature of  $\sim 550$  °C for Allende (43) being significantly lower than the Hf–W closure temperature of  $\sim 800$ – $900$  °C (44) and is further supported by the minimal redistribution of elements between matrix and chondrules, even for aqueously mobile elements such as Sr (11). Thus, parent body processes also had no significant effect on the  $^{182}\text{Hf}-^{182}\text{W}$  systematics, meaning that the Hf–W chondrule–matrix isochron provides the time of chondrule formation. Furthermore, bulk CAIs from Allende plot on a well-defined Hf–W isochron (20), whose slope is significantly steeper than that of the chondrule–matrix isochron; the preservation of two distinct Hf–W isochrons for different components in Allende indicates that these systematics remained largely unaffected by parent body processes. Finally, we note that the Hf–W age we obtained for Allende chondrules is in excellent agreement with other chronological data for the formation age of Allende chondrules, providing further support that the Hf–W isochron dates the formation of Allende chondrules.

**S2.6. Comparison with Previous Studies.** A recent study also reported Hf–W data for chondrule and matrix separates from the Allende meteorite (18). The chondrule fractions analyzed in this previous study consisted of only 5–75 chondrules, corresponding to total weights of 12–48 mg; matrix separates ranged between 9 and 22 mg. Based on the reported W concentrations, the matrix and chondrule separates provided only  $\sim 1$ – $5$  ng W for the W isotope measurements, leading to large inherent uncertainties on the measured W isotope ratios (about  $\pm 0.5$   $\epsilon$  units). Nevertheless, the previous study reported a Hf–W age of  $-1.2 \pm 3.0$  Ma after CAI formation for different Allende components, including chondrules and matrix. This age was obtained after correcting the measured  $\epsilon^{182}\text{W}$  values not only for nucleosynthetic isotope anomalies but also for large organic interferences on  $^{183}\text{W}$ . Note

that these organic interferences are highly variable and can be fairly large (up to several  $\epsilon$  units). For this reason, Becker et al. (18) used the  $\epsilon^{182}\text{W}$  (6/4) values for the chronological interpretation of their Hf-W data, because this normalization is not affected by the organic interferences. However, the 6/4-normalized data require a large correction for nucleosynthetic anomalies (up to several  $\epsilon$  units), which in turn requires accurate  $\epsilon^{183}\text{W}$  (6/4) values. The  $\epsilon^{183}\text{W}$  values reported by Becker et al. (18) are compromised by the occurrence of organic interferences on  $^{183}\text{W}$  for at least some of the investigated samples, however. To overcome this problem, these authors “corrected” the organic interferences on  $\epsilon^{183}\text{W}$  (6/4) by shifting the data points along the  $x$  axis in the  $\epsilon^{182}\text{W}_i$  vs.  $\epsilon^{183}\text{W}$  (6/4) plot until the points intercept with the theoretical correlation line for nucleosynthetic isotope variations. For the slope of this correlation line, the authors used a value of 1.673, but this value is derived from an outdated theoretical model of stellar  $s$ -process nucleosynthesis; using the most recent models and also W isotope data for CAIs and acid leachates from primitive meteorites results in significantly shallower slopes of between 1.23 and 1.54 (for details, see ref. 17). Thus, the correction procedure in Becker et al. (18) for both the organic interferences and nucleosynthetic isotope anomalies is incorrect, resulting in spuriously corrected  $\epsilon^{182}\text{W}$  (6/4) values. Obviously, for the proper interpretation of the chondrule and matrix data, accurate  $^{183}\text{W}$  data free of organic interferences are necessary. Note that Becker et al. (18) have empirically defined a  $\epsilon^{182}\text{W}_i - \epsilon^{183}\text{W}$  (6/4) slope for their data (excluding samples with obvious organic interferences) of about  $1.3 \pm 0.6$ ; this value is consistent with the slope defined in the present study but also has a very large uncertainty, making the correction of the Becker et al. (18) data for nucleosynthetic isotope anomalies very uncertain.

The improper correction for nucleosynthetic isotope anomalies used by Becker et al. (18) ultimately leads to an inaccurate calculated Hf-W age. Note that the presence of organic interferences on  $^{183}\text{W}$  in the data set of Becker et al. (18) makes the correction of nucleosynthetic anomalies nearly impossible, because the magnitude of nucleosynthetic  $^{183}\text{W}$  excesses and deficits cannot be quantified reliably. For instance, a sample with a small measured  $^{183}\text{W}$  excess could in fact be characterized by a nucleosynthetic  $^{183}\text{W}$  deficit with a superimposed organic  $^{183}\text{W}$  interference. Nevertheless, if we correct the data of the previous study using the  $\epsilon^{182}\text{W}_i(6/4) - \epsilon^{183}\text{W}(6/4)$  slope derived from our much more precise W isotope data, we obtain an age of  $4 \pm 7$  Ma after CAIs (where samples with obvious organic interferences are excluded and all samples are corrected for nucleosynthetic

anomalies) that is  $\sim 5$  Ma younger than the age originally reported by Becker et al. (18). This revised age is within its large uncertainty consistent with the precise age of  $2.2 \pm 0.8$  Ma after CAIs obtained based on our Hf-W data for Allende chondrules and matrix. We conclude that the disparity in ages between our and the Becker et al. (18) study is attributable to the improper correction for nucleosynthetic isotope anomalies combined with large analytical artifacts on  $^{183}\text{W}$  in the latter study.

In contrast to the previous study, we analyzed much larger amounts of chondrules and matrix, which are required to obtain W isotope data of sufficient precision. The chondrule fractions analyzed in this study consisted of 155 to  $\sim 3,000$  chondrules and chondrule fragments (Table S1), corresponding to total weights of  $\sim 300$ – $500$  mg; matrix separates ranged between  $\sim 400$  and  $\sim 500$  mg. Consequently, the amount of W available for the W isotope measurements was an order of magnitude higher than in the previous study. Our sample set, therefore, allows to measure large amounts of W ( $\sim 30$  ng of W per analysis), yielding W isotope ratios with the required precision (i.e., external reproducibility of about  $\pm 0.1$   $\epsilon$  units). Moreover, our data are not compromised by any organic interferences on  $^{183}\text{W}$ , as has been verified by repeated measurements of several terrestrial standards (Table S2) and bulk Allende samples. We observed a small mass-independent effect on  $^{183}\text{W}$  ( $\sim 0.1$   $\epsilon$  units), which has been reliably quantified by repeated analyses of several digestion aliquots of the terrestrial rock standard BHVO-2 and corrected for all samples (*S1. SI Materials and Methods, S1.2. Chemical Separation and W Isotope Measurements*). We note, however, that this effect is an order of magnitude smaller than the observed nucleosynthetic  $^{183}\text{W}$  anomalies and, thus, does not compromise any of the interpretations made in the present study.

In summary, we note that highly precise and accurate W isotope data (including normalizations involving  $^{183}\text{W}$ ) are necessary to properly resolve and assess nucleosynthetic isotope anomalies in chondrules and matrix. Only then is it possible to not rely on theoretical models of  $s$ -process nucleosynthesis but to empirically constrain the effect of nucleosynthetic anomalies on measured  $\epsilon^{182}\text{W}$  values, as accomplished in the present study. Such an empirical correction is necessary, because as shown by our data, nucleosynthetic isotope anomalies can have different origins, such that the correction for these anomalies cannot be done assuming one constant  $\epsilon^{182}\text{W}/\epsilon^{183}\text{W}$  ratio. Thus, only if the nucleosynthetic isotope anomalies are corrected empirically, is it possible to obtain an accurate Hf-W age for chondrules and matrix.

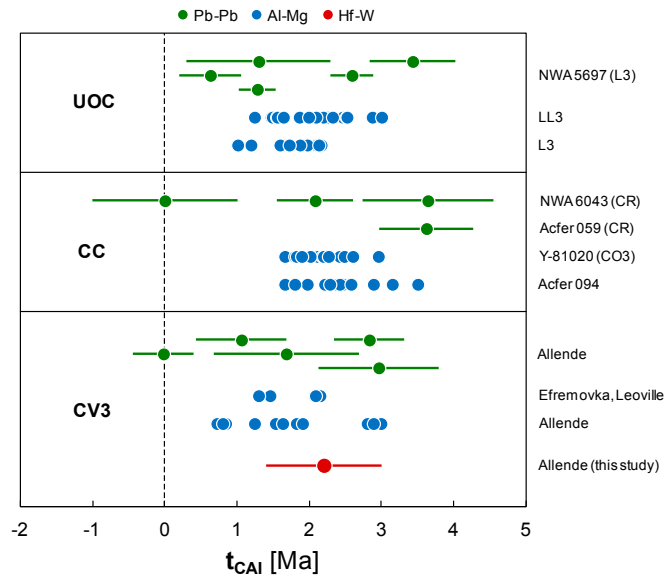


**Fig. S1.** Al-Mg and Pb-Pb ages for individual chondrules from carbonaceous (CC) and unequilibrated ordinary (UOC) chondrites range between ~0 and ~3.5 Ma after CAI formation, although most chondrules have ages close to 2 Ma. Given the large number of chondrules and chondrule fragments analyzed in this study (~5,000), the obtained Hf-W age of  $2.2 \pm 0.8$  Ma after CAI formation corresponds to the time at which the majority of Allende chondrules formed. Sources of Pb-Pb ages are provided in ref. 45 and calculated relative to  $t_0 = 4567.3$  Ma (14). Ages before 2010 are U-corrected using  $^{238}\text{U}/^{235}\text{U} = 137.786$  (45). Al-Mg ages are from refs. 28 and 29 and references therein.

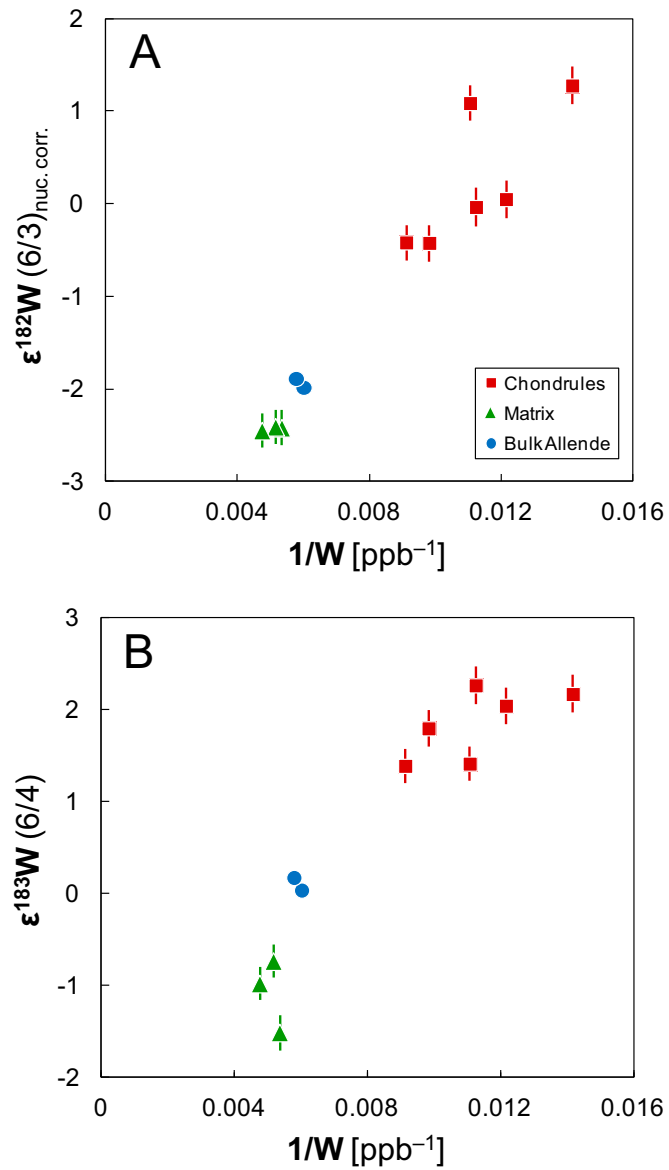


**Fig. 52.**  $\epsilon^{182}\text{W}$  (A) and  $\epsilon^{183}\text{W}$  (B) vs.  $1/W$  plots showing that the different chondrule and matrix fractions do not reflect simple two-component mixing. The absence of a well-defined linear correlation between  $\epsilon^{182}\text{W}$  and  $1/W$  implies that the Hf-W isochron obtained for Allende chondrules and matrix (Fig. 2B) has chronological significance.



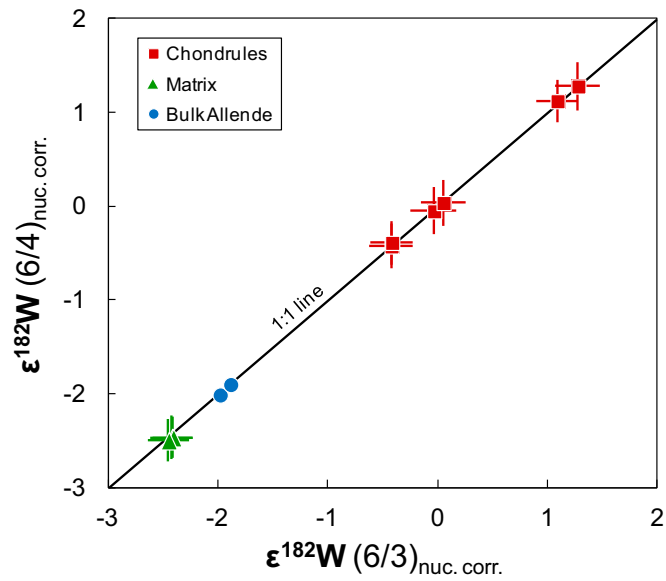


**Fig. S4.**  $\epsilon^{182}\text{W} (6/4)$  vs.  $\epsilon^{182}\text{W} (6/3)$  of Allende chondrules and matrix after correction for nucleosynthetic anomalies. Both normalizations yield consistent results, but the precision of the 6/3-normalized values is generally better because of much smaller corrections for nucleosynthetic W isotope anomalies. Note that bulk Allende was not included in the correction procedure but plots on the same correlation line when corrected as chondrules and matrix separates.



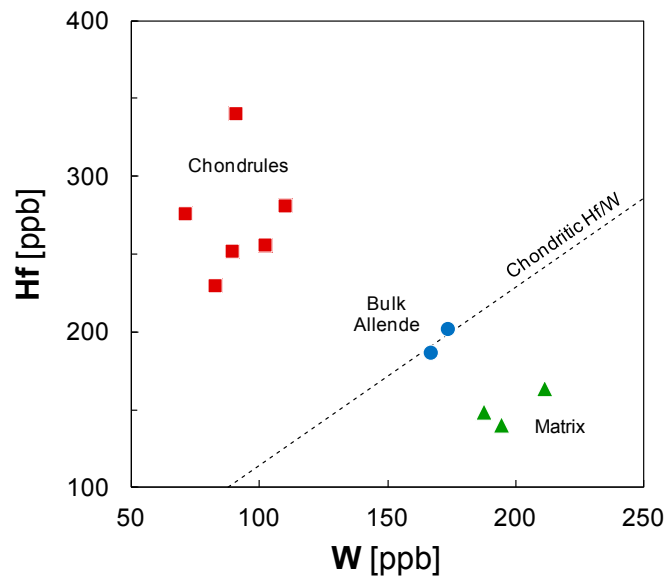


**Fig. S6.** Hf and W concentrations of chondrule and matrix separates from Allende, which show complementary Hf-W systematics. Note that Hf contents of the chondrule fractions vary depending on their grain size and that the spread in W concentrations is largely attributable to the magnetic separation of fraction C3. The dashed line represents the average Hf/W of carbonaceous chondrites (16).

**Table S1. Description of samples prepared and analyzed in this study**

Sample	Grain size, $\mu\text{m}$	<i>N</i>	Description	Weight, mg
Chondrule fractions				
C1	250–1,600	ND	F&T	302
C2	1,000–1,600	155		483
C3m	500–1,000	~465	High MS	384
C3n	500–1,000	~915	Low MS	493
C3i	500–1,000	~760	Intermediate MS	518
C4	250–500	~3,000		527
Matrix separates				
M1	Suspension	—	F&T	506
M2	250–500	—	Hand-picked	394
M3	Suspension	—	Ultrasonic.	469
Bulk Allende				
MS-A	Powder	—	From ~100-g slab	~500 (6 $\times$ )
MS-B	Powder	—	From ~40-g slab	~500 (7 $\times$ )
Terrestrial standard				
BHVO-2	Powder	—		~500 (12 $\times$ )

The two bulk Allende powders and BHVO-2 were digested multiple times. Note that an additional ~50 mg was recovered for fraction C3i that was not digested. See *S1. SI Materials and Methods, S1.1. Sample Preparation* for additional information. F&T, freeze–thaw disaggregation; MS, magnetic susceptibility; *N*, no. of chondrules and chondrule fragments; ND, not determined.

**Table S2. Hf-W data for the terrestrial rock standard BHVO-2**

ID	Hf ng/g	W ng/g	Normalized to $^{186}\text{W}/^{184}\text{W} = 0.92767$			Normalized to $^{186}\text{W}/^{183}\text{W} = 1.98590$			
			$\epsilon^{182}\text{W}_{\text{meas.}}$ $\pm 2 \text{ SE}$	$\epsilon^{183}\text{W}_{\text{meas.}}$ $\pm 2 \text{ SE}$	$\epsilon^{183}\text{W}_{\text{corr.}}^*$ $\pm 2\sigma$	$\epsilon^{182}\text{W}_{\text{meas.}}$ $\pm 2 \text{ SE}$	$\epsilon^{182}\text{W}_{\text{corr.}}^*$ $\pm 2\sigma$	$\epsilon^{184}\text{W}_{\text{meas.}}$ $\pm 2 \text{ SE}$	$\epsilon^{184}\text{W}_{\text{corr.}}^*$ $\pm 2\sigma$
BHV01.1	4,535	215	-0.01 ± 0.08	-0.04 ± 0.07	0.04 ± 0.10	0.11 ± 0.06	0.06 ± 0.11	0.02 ± 0.05	-0.03 ± 0.08
BHV01.2	—	—	-0.08 ± 0.09	-0.16 ± 0.09	-0.05 ± 0.12	0.15 ± 0.08	-0.07 ± 0.14	0.11 ± 0.06	0.03 ± 0.10
BHV01.3	—	—	-0.07 ± 0.08	-0.09 ± 0.07	-0.04 ± 0.10	0.08 ± 0.07	-0.05 ± 0.11	0.06 ± 0.04	0.02 ± 0.09
BHV02.1	—	—	0.00 ± 0.08	-0.04 ± 0.07	0.00 ± 0.10	0.06 ± 0.06	0.01 ± 0.12	0.03 ± 0.05	0.00 ± 0.08
BHV02.2	—	—	0.04 ± 0.08	-0.08 ± 0.07	0.02 ± 0.10	0.14 ± 0.07	0.04 ± 0.12	0.05 ± 0.05	-0.02 ± 0.09
BHV02.3	—	—	-0.03 ± 0.07	-0.10 ± 0.07	-0.01 ± 0.11	0.12 ± 0.07	-0.02 ± 0.13	0.06 ± 0.05	0.01 ± 0.09
BHV03.1	4,540	219	-0.01 ± 0.08	-0.09 ± 0.07	0.00 ± 0.11	0.13 ± 0.07	0.00 ± 0.12	0.06 ± 0.05	0.00 ± 0.09
BHV03.2	—	—	-0.03 ± 0.08	-0.20 ± 0.07	-0.04 ± 0.10	0.23 ± 0.07	-0.05 ± 0.12	0.13 ± 0.05	0.02 ± 0.09
BHV04.1	—	—	0.08 ± 0.09	-0.01 ± 0.08	0.07 ± 0.11	0.11 ± 0.06	0.10 ± 0.13	0.01 ± 0.05	-0.05 ± 0.09
BHV04.2	—	—	-0.07 ± 0.08	-0.16 ± 0.07	-0.12 ± 0.10	0.06 ± 0.07	-0.16 ± 0.12	0.10 ± 0.05	0.08 ± 0.09
BHV05.1	4,445	212	-0.07 ± 0.09	-0.12 ± 0.08	-0.06 ± 0.11	0.09 ± 0.07	-0.08 ± 0.14	0.08 ± 0.06	0.04 ± 0.10
BHV05.2	—	—	0.01 ± 0.09	-0.11 ± 0.07	-0.02 ± 0.10	0.13 ± 0.06	-0.02 ± 0.12	0.07 ± 0.05	0.01 ± 0.08
BHV06.1	—	—	-0.01 ± 0.08	-0.10 ± 0.07	0.02 ± 0.11	0.17 ± 0.07	0.03 ± 0.12	0.06 ± 0.05	-0.01 ± 0.09
BHV06.2	—	—	-0.08 ± 0.08	-0.25 ± 0.07	-0.08 ± 0.10	0.26 ± 0.06	-0.10 ± 0.12	0.17 ± 0.05	0.05 ± 0.08
BHV07.1	4,503	215	-0.02 ± 0.07	-0.17 ± 0.07	-0.07 ± 0.09	0.14 ± 0.06	-0.09 ± 0.11	0.11 ± 0.04	0.04 ± 0.08
BHV07.2	—	—	-0.07 ± 0.08	-0.13 ± 0.07	-0.03 ± 0.10	0.14 ± 0.07	-0.04 ± 0.11	0.09 ± 0.04	0.02 ± 0.08
BHV07.3	—	—	-0.04 ± 0.09	-0.10 ± 0.06	-0.06 ± 0.10	0.05 ± 0.08	-0.08 ± 0.11	0.06 ± 0.04	0.04 ± 0.09
BHV08.1	—	—	0.11 ± 0.10	-0.11 ± 0.09	0.03 ± 0.12	0.20 ± 0.07	0.05 ± 0.14	0.07 ± 0.06	-0.02 ± 0.10
BHV08.2	—	—	-0.04 ± 0.11	-0.14 ± 0.09	-0.02 ± 0.14	0.17 ± 0.10	-0.02 ± 0.16	0.09 ± 0.06	0.01 ± 0.12
BHV08.3	—	—	0.09 ± 0.09	-0.03 ± 0.07	0.02 ± 0.11	0.07 ± 0.08	0.02 ± 0.13	0.02 ± 0.05	-0.01 ± 0.10
BHV09.1	4,471	213	-0.02 ± 0.10	-0.21 ± 0.08	-0.04 ± 0.12	0.24 ± 0.08	-0.06 ± 0.14	0.14 ± 0.05	0.03 ± 0.10
BHV09.2	—	—	-0.05 ± 0.08	-0.16 ± 0.08	-0.01 ± 0.12	0.21 ± 0.08	-0.01 ± 0.14	0.11 ± 0.05	0.00 ± 0.10
BHV09.3	—	—	0.09 ± 0.09	-0.14 ± 0.08	0.05 ± 0.12	0.28 ± 0.07	0.08 ± 0.14	0.10 ± 0.05	-0.04 ± 0.10
BHV10.1	—	—	-0.04 ± 0.09	-0.19 ± 0.08	-0.05 ± 0.12	0.21 ± 0.08	-0.06 ± 0.14	0.13 ± 0.05	0.03 ± 0.10
BHV10.2	—	—	-0.08 ± 0.09	-0.19 ± 0.08	-0.05 ± 0.11	0.20 ± 0.07	-0.07 ± 0.13	0.13 ± 0.05	0.03 ± 0.10
BHV11.1	4,570	217	-0.06 ± 0.08	-0.13 ± 0.07	-0.05 ± 0.11	0.12 ± 0.07	-0.06 ± 0.12	0.09 ± 0.05	0.03 ± 0.09
BHV11.2	—	—	-0.09 ± 0.08	-0.17 ± 0.07	-0.09 ± 0.11	0.12 ± 0.07	-0.12 ± 0.12	0.11 ± 0.05	0.06 ± 0.09
BHV12.1	—	—	-0.06 ± 0.09	-0.09 ± 0.10	-0.02 ± 0.13	0.10 ± 0.08	-0.03 ± 0.16	0.06 ± 0.07	0.02 ± 0.11
BHV12.2	—	—	0.00 ± 0.08	-0.21 ± 0.07	-0.03 ± 0.10	0.25 ± 0.07	-0.04 ± 0.12	0.14 ± 0.05	0.02 ± 0.09
<i>n</i>	6	6	29	29	29	29	29	29	29
Mean	4,511	215	-0.02	-0.13	-0.02	0.15	-0.03	0.09	0.01
2 SD	93	5.4	0.11	0.12	0.09	0.13	0.12	0.08	0.06
95% CI	49	2.8	0.02	0.02	0.02	0.02	0.02	0.02	0.01

Different numbers (01–12) denote separate digestions of ~0.5 g standard powder that were processed through full chemical separation procedure and analyzed with each set of samples. \*W isotope ratios involving  $^{183}\text{W}$  are corrected for a small mass-independent effect (*S1. SI Materials and Methods, S1.2. Chemical Separation and W Isotope Measurements*).



**Table S4. Isochron regressions and corresponding ages for the investigated Allende samples**

Samples	N	Normalized to $^{186}\text{W}/^{184}\text{W}$ (6/4)				Normalized to $^{186}\text{W}/^{183}\text{W}$ (6/3)			
		$\epsilon^{182}\text{W}_i$	$^{182}\text{Hf}/^{180}\text{Hf}_i$ ( $\times 10^{-5}$ )	MSWD	$\Delta t_{\text{CAI}}$ (Ma, $\pm 2\sigma$ )	$\epsilon^{182}\text{W}_i$	$^{182}\text{Hf}/^{180}\text{Hf}_i$ ( $\times 10^{-5}$ )	MSWD	$\Delta t_{\text{CAI}}$ (Ma, $\pm 2\sigma$ )
Using measured $\epsilon^{182}\text{W}$ values									
Chondrules	6					$-3.59 \pm 0.40$	$8.84 \pm 0.94$	0.48	$1.81 \pm 1.47$
Chondrules + matrix	9					$-3.21 \pm 0.13$	$7.98 \pm 0.36$	0.87	$3.13 \pm 0.80$
Chondrules + matrix + bulk rock	11					$-3.19 \pm 0.06$	$7.94 \pm 0.27$	0.87	$3.19 \pm 0.70$
Using $\epsilon^{182}\text{W}$ values corrected for nucleosynthetic W isotope anomalies									
Chondrules	6	$-3.49 \pm 0.54$	$8.96 \pm 1.3$	0.24	$1.64 \pm 1.94$	$-3.46 \pm 0.44$	$8.87 \pm 1.0$	0.50	$1.77 \pm 1.55$
Chondrules + matrix	9	$-3.40 \pm 0.16$	$8.74 \pm 0.48$	0.21	$1.96 \pm 0.89$	<b><math>-3.34 \pm 0.13</math></b>	<b><math>8.58 \pm 0.39</math></b>	0.45	<b><math>2.20 \pm 0.80</math></b>
Chondrules + matrix + bulk rock	11	$-3.29 \pm 0.07$	$8.54 \pm 0.36$	0.87	$2.26 \pm 0.77$	$-3.27 \pm 0.06$	$8.44 \pm 0.30$	0.76	$2.41 \pm 0.71$

Isochrons were calculated using Isoplot version 3.76 (Model 1 fit). Unless otherwise stated, uncertainties represent 95% CIs. Best estimates are shown in bold. See S2. SI Text, S2.4. Isochron Regression and Chronological Significance for details. MSWD, mean square of weighted deviates; N, no. of samples included.